BNL-NUREG-27834
INFORMAL REPORT
LIMITED DISTRIBUTION

NONLINEAR DYNAMIC ANALYSIS OF PIPING SYSTEM USING THE PSEUDO FORCE METHOD

By

P. Bezler and S. Prachuktam
Structural Analysis Group
Department of Nuclear Energy
Brookhaven National Laboratory
Upton, NY 11973

and

M. Hartzman
Division of Systems Safety
U. S. Nuclear Regulatory Commission
Bethesda, MD 20014

ABSTRACT

Simple piping systems are composed of linear elastic elements and can be analyzed using conventional linear methods. The introduction of constraint springs separated from the pipe with clearance gaps to such systems to cope with the pipe whip or other extreme excitation conditions introduces nonlinearities to the system, the nonlinearities being associated with the gaps. Since these spring-damper constraints are usually limited in number, discretely located, and produce only weak nonlinearities, the analysis of linear systems including these nonlinearities can be carried out by using modified linear methods. In particular, the application of pseudo force methods wherein the nonlinearities are treated as displacement dependent forcing functions acting on the linear system were investigated.

The nonlinearities induced by the constraints were taken into account as generalized pseudo forces on the right-hand side of the governing dynamic equilibrium equations. Then an existing linear elastic finite element piping code, EPIPE, was modified to permit application of the procedure. This option was inserted such that the analyses could be performed using either the direct integration method or via a modal superposition method, the Newmark-Beta integration procedure being employed in both methods. The modified code was proof tested against several problems taken from the literature or developed with the nonlinear dynamics code OSCIL. The problems included a simple pipe loop, a cantilever beam, and a lumped mass system subjected to pulsed and periodic forcing functions. The problems were selected to gage the overall accuracy of the method and to insure that it properly predicted the jump phenomena associated with nonlinear systems.

Implementation of the method was found to be straightforward with the simplest iteration procedure for the psuedo force vector sufficing. The results predicted with the method agreed in all important aspects with existing solutions as well as those generated with other methods. With linear analyses, the modal superposition solution mode was found to be the most efficient, however, exhibiting slightly greater inaccuracies.

CONTENTS

I. Introduction

Simple piping systems are composed of linear elastic elements and can be analyzed using conventional linear methods. The introduction of constraint springs (bumpers) separated from the pipe with clearance gaps to such systems to cope with pipe whip or other extreme excitation conditions introduces nonlinearities to the system. The nonlinearities are produced by the clearance gaps in the bumper assemblies and additionally by the nonlinear stiffness of the bumper springs. Since these spring-damper assemblies are usually limited in number, discretely located, and produce only weak nonlinearities, the analysis of linear systems including these can be carried out by using modified linear methods. In particular, the application of pseudo force methods wherein the nonlinearities are treated as displacement dependent forcing functions acting on the linear system were investigated.

To perform the investigation an available linear elastic finite element code was modified to accommodate the method. Solutions to several problems were developed and compared to existing solutions and or to solutions developed using a general purpose nonlinear analysis code. The relative merits and accuracy of the method were then determined by comparison.

II. System Equations and Method Implementation

The nonlinearities induced by the bumpers are taken into account as generalized pseudo forces on the right-hand side of the governing dynamic equilibrium equations as

$$[M]\,[\ddot{W}] + [C]\,[\dot{W}] + [K]\,[W] = [F] + [P] \qquad (1)$$

where

[M], [C], and [K] are the mass, damping, and stiffness matrices,

[W], [$\dot{W}$], and [$\ddot{W}$] are the displacement, velocity, and acceleration vectors,

[F] is the external load vector, and

[P] is the pseudo force vector of nonlinear external forces due to bumpers. The pseudo forces can be calculated as:

$$P_i^n(u_i, \dot{u}_i) = k_i^n (u_i^n - g_i^n) + c_i^n \dot{u}_i^n \qquad \text{if } u_i^n > g_i^n \tag{2}$$

$$= 0 \qquad \text{if } u_i^n \leq g_i^n$$

where the superscript n and subscript i connotate node n in the i^{th} direction. k_i, c_i, and g_i are the spring constants, damping coefficients, and clearance gaps of the bumpers.

The dynamic equilibrium equation (1) can be solved by either the direct integration procedure[1] or normal mode theory.[2] Both methods will be considered below.

II.1 The Direct Integration Method

Since the nonlinearities are treated as pseudo forces, the left-hand side of Eq. (1) remains linear and must be formed and triangulized only once. The solution at each time step can be obtained by backward substitution. The selection of the integration procedure is based on the fact that for these systems, the action of the higher modes of motion may strongly influence the displacements at the nonlinear elements and thereby define the pseudo force magnitudes. Since most numerical integration schemes introduce artificial damping into the system and since damping has a disproportionate effect on the higher modes, the selection was based on the level of artificial damping associated with each method. Of the methods surveyed, the Newmark-Beta method, has no artificial damping associated with it and this was the method used in

these procedures. All the other methods, such as central difference, Houbolt method, and Wilson-θ method introduce artifical damping in varying amounts, with the Wilson-θ method introducing the most.[3]

The assumptions used on the Newmark integration scheme are

$$\dot{W}_{t+\Delta t} = \dot{W}_t + [(1-\delta)\ddot{W}_t + \delta\ddot{W}_{t+\Delta t}]\Delta t \tag{3}$$

$$W_{t+\Delta t} = W_t + \dot{W}_t \Delta t + [(1/2-\alpha)\ddot{W}_t + \alpha\ddot{W}_{t+\Delta t}]\Delta t^2 \tag{4}$$

where α and δ are parameters that can be selected to achieve integration accuracy and stability. The suggested values are $\delta = 1/2$ and $\alpha = 1/4$.

The equilibrium equation (1) at time $t+\Delta t$ is

$$[M]\ [\ddot{W}_{t+\Delta t}] + [C]\ [\dot{W}_{t+\Delta t}] + [K]\ [W_{t+\Delta t}] = [F_{t+\Delta t}] + [P_{t+\Delta t}] \tag{5}$$

Using Eqs. (3) and (4), equation (5) may be expressed in terms of $W_{t+\Delta t}$ as

$$[K^{eff}]\ [W_{t+\Delta t}] = [F^{eff}] \tag{6}$$

where

$$[K^{eff}] = [K] + A_o[M] + A_1[C] \tag{7}$$

and

$$[F^{eff}] = [F_{t+\Delta t}] + [P_{t+\Delta t}] + [M]\ \{A_o[W_t] + A_2[\dot{W}_t] + A_3\ [\ddot{W}_t]\}$$

$$+ C\ \{A_1[W_t] + A_4[\dot{W}_t] + A_5[\ddot{W}_t]\} \qquad (8)$$

with

$$A_o = \frac{1}{\alpha\Delta t^2} \qquad A_4 = \frac{\delta}{\alpha} - 1$$

$$A_1 = \frac{\delta}{\alpha\Delta t} \qquad A_5 = \frac{\Delta t}{2}\left(\frac{\delta}{\alpha} - 2\right)$$

$$A_2 = \frac{1}{\alpha\Delta t} \qquad A_6 = \Delta t\ (1-\delta) \qquad (9)$$

$$A_3 = \frac{1}{2\alpha} - 1 \qquad A_7 = \delta\Delta t$$

As indicated in (8) $[F^{eff}]$ is dependent on $[P_{t+\Delta t}]$, an unknown vector which is in general a function of $W(t+\Delta t)$ and $\dot{W}(t+\Delta t)$. The procedure we use to estimate $[P_{t+\Delta t}]$, is as follows:

1) Estimate $W_{t+\Delta t}$ assuming $[P_{t+\Delta t}] = 0$ i.e., compute $[Y_o]$ where

$$[K^{eff}]\ [Y_o] = [F_{t+\Delta t}] + [M]\ \{A_o[W_t] + A_2[\dot{W}_t] + A_3[\ddot{W}_t]\}$$

$$+ [C]\ \{A_1[W_t] + A_4[\dot{W}_t] + A_5[\ddot{W}_t]\}$$

2) Compute bumper forces corresponding to Y_o

$$[P_{t+\Delta t}] = [K_s]\,[Y_o] + [C_s]\,[\dot{Y}_o]$$

where $[K_s]$ is the matrix of bumper spring constants and $[C_s]$ is the matrix of bumper damping coefficients.

3) Compute the additional displacement corresponding to these bumper forces

$$[B] = [K^{eff}]^{-1}\,[P_{t+\Delta t}]$$

4) Estimate $W_{t+\Delta t}$ as

$$[Y_{t+\Delta t}] = [Y_o] + [B]$$

This procedure can be repeated until the difference $(W_{t+\Delta t}^{N} - W_{t+\Delta t}^{N-1})$ achieves some tolerance. We have found that iteration does not strongly effect the results and is not warranted. The solutions are obtained by following steps 1 thru 4 without iteration. The identical procedure is also followed in the normal mode method.

II.2 The Normal Mode Method

For this method, the natural frequencies and the associated mode shapes for the system are computed first, then the equilibrium equation, Eq. (1) is transformed to the generalized eigen problem by using the following transformation:

$$W(t) = \phi x(t) \tag{10}$$

where

$W(t)$ = the vector of the displacements

ϕ_i = the i^{th} mode shape vector

$X(t)$ = the vector of the generalized displacements

Defining a matrix Φ whose columns are the eigenvectors ϕ_i and a diagonal matrix Ω^2 which stores the eigenvalues ω_i^2 on its diagonal

$$\Phi = [\phi_1, \phi_2, \phi_3, \cdots \phi_n] \qquad \Omega^2 = \begin{bmatrix} \omega_1^2 & & & & \\ & \ddots & & & \\ & & \omega_i^2 & & \\ & & & \ddots & \\ & & & & \omega_n^2 \end{bmatrix} \tag{11}$$

Since the eigenvectors are M-orthonormal, we have

$$\Phi^T K \Phi = \Omega^2 \tag{12}$$

and

$$\Phi^T M \Phi = I \text{ where I is the identity matrix} \tag{13}$$

$$\Phi^T C \Phi = \text{diag. } (2w_i \xi_i) \tag{14}$$

where

ξ_i is the damping ratio in the i^{th} mode.

Eq. (1) becomes:

$$\ddot{X}(t) + \nabla\dot{X}(t) + \Omega^2 X(t) = \Phi^T F + \Phi^T P \tag{15}$$

where

∇ = the diagonal matrix of $2\omega_i\xi_i$

i=1, total number of modes

Ω^2 = the diagonal matrix of ω_i^2

i=1, total number of modes

The system of equations in Eq. (15) are decoupled, so the solutions of the generalized displacements can be obtained by time integration without the inversion of the effective stiffness.

The time integration used is again the Newmark-Beta method, where the equilibrium equation, Eq. (15) is considered at time t+Δt, we have

$$\begin{bmatrix} \ddot{X}_{t+\Delta t} \\ \dot{X}_{t+\Delta t} \\ X_{t+\Delta t} \end{bmatrix} = A \begin{bmatrix} \ddot{X}_t \\ \dot{X}_t \\ X_t \end{bmatrix} + L[f_{t+\Delta t}] + L[p_{t+\Delta t}] \tag{16}$$

where

$$A = \begin{bmatrix} -(1/2-\alpha)\beta-2(1-\delta)K & \frac{1}{\Delta t}(-\beta-2K) & \frac{1}{\Delta t^2}(-\beta) \\ \Delta t[1-\delta-(1/2-\alpha)\delta\beta-2(1-\delta)\delta K & 1-\beta\delta-2\delta K & \frac{1}{\Delta t}(-\beta\delta) \\ \Delta t^2[1/2-\alpha-(1/2-\alpha)\alpha\beta-2(1-\delta)\alpha K & \Delta t(1-\alpha\beta-2\alpha K) & (1-\alpha\beta) \end{bmatrix} \tag{17}$$

$$\beta = \left(\frac{1}{\omega^2\Delta t^2} + \frac{2\xi\delta}{\omega\Delta t} + \alpha\right)^{-1} \qquad K = \frac{\xi\beta}{\omega\Delta t} \tag{18}$$

$$L = \begin{bmatrix} \frac{\beta}{\omega^2\Delta t^2} \\ \frac{\beta\delta}{\omega^2\Delta t} \\ \frac{\alpha\beta}{\omega^2} \end{bmatrix} \tag{19}$$

$f_{t+\Delta t}$ is the modal load due to external loads at time $t+\Delta t$ and

$P_{t+\Delta t}$ is the modal load due to bumper forces at time $t+\Delta t$.

The actual time responses of the structure are:

$$\begin{aligned} W(t) &= \phi X(t) \\ \dot{W}(t) &= \phi \dot{X}(t) \\ \ddot{W}(t) &= \phi \ddot{X}(t) \end{aligned} \tag{20}$$

Note that this scheme is restricted to small time steps to assure a required level of accuracy. Normally, a time step of 1/10 of the smallest period of the system is recommended. Moreover, in the selection of the necessary number of modes, all modes which influence the motions at the nonlinear elements must be considered.

Both the direct integration option and the normal mode option were incorporated into an existing linear finite element code EPIPE. This required the addition of some simple algorithms and the substitution of the Newmark-Beta integration scheme for the original integration algorithm. These modifications were most readily made for the direct integration solution mode while requiring some additional coding for the modal superposition solution mode (gap effects necessitated a constant return to system coordinates). However, overall the implementation was found to be straight forward.

III. Numerical Examples

Four separate problems were used to evaluate the method. For two, solutions were available in the literature permitting an independent check while for the remaining two solutions were developed using the nonlinear analysis code OSCIL.[6] The problems were chosen to simulate piping systems and to test the capacity of the method to predict salient nonlinear characteristics.

III.1 Three Dimensional Coolant Loop

For the first example, a three-dimensional nonlinear piping system, shown in Figure 1, consisting of nine straight pipes and two elbows with three gap-bumper supports was considered. The system was subjected to the dynamic loads shown in Figure 2. Solutions to this problem by two techniques are given in Reference 2 and are presented in Figure 3 of this report.

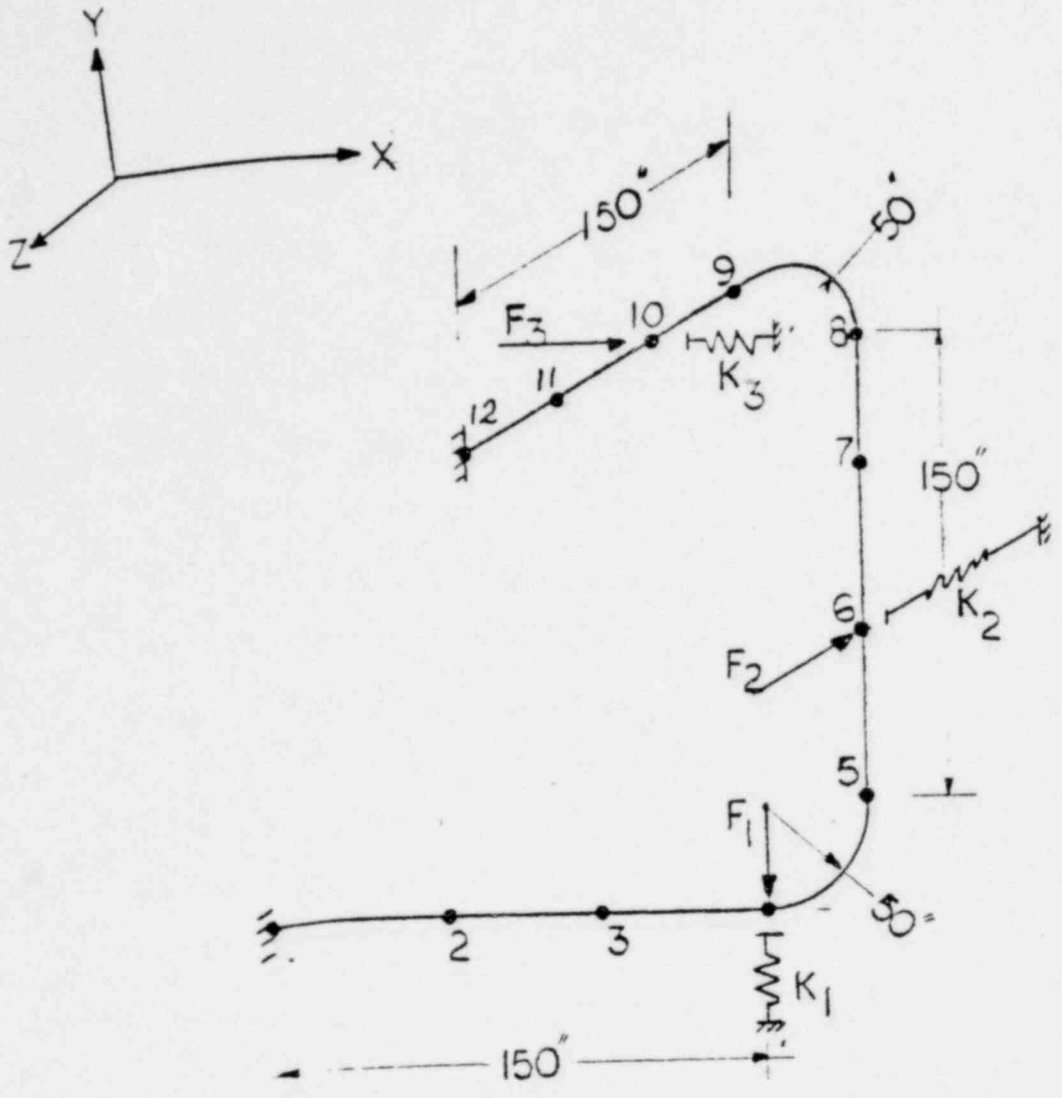

FIG.1 3-D PIPING SYSTEM W/GAP-BUMPERS

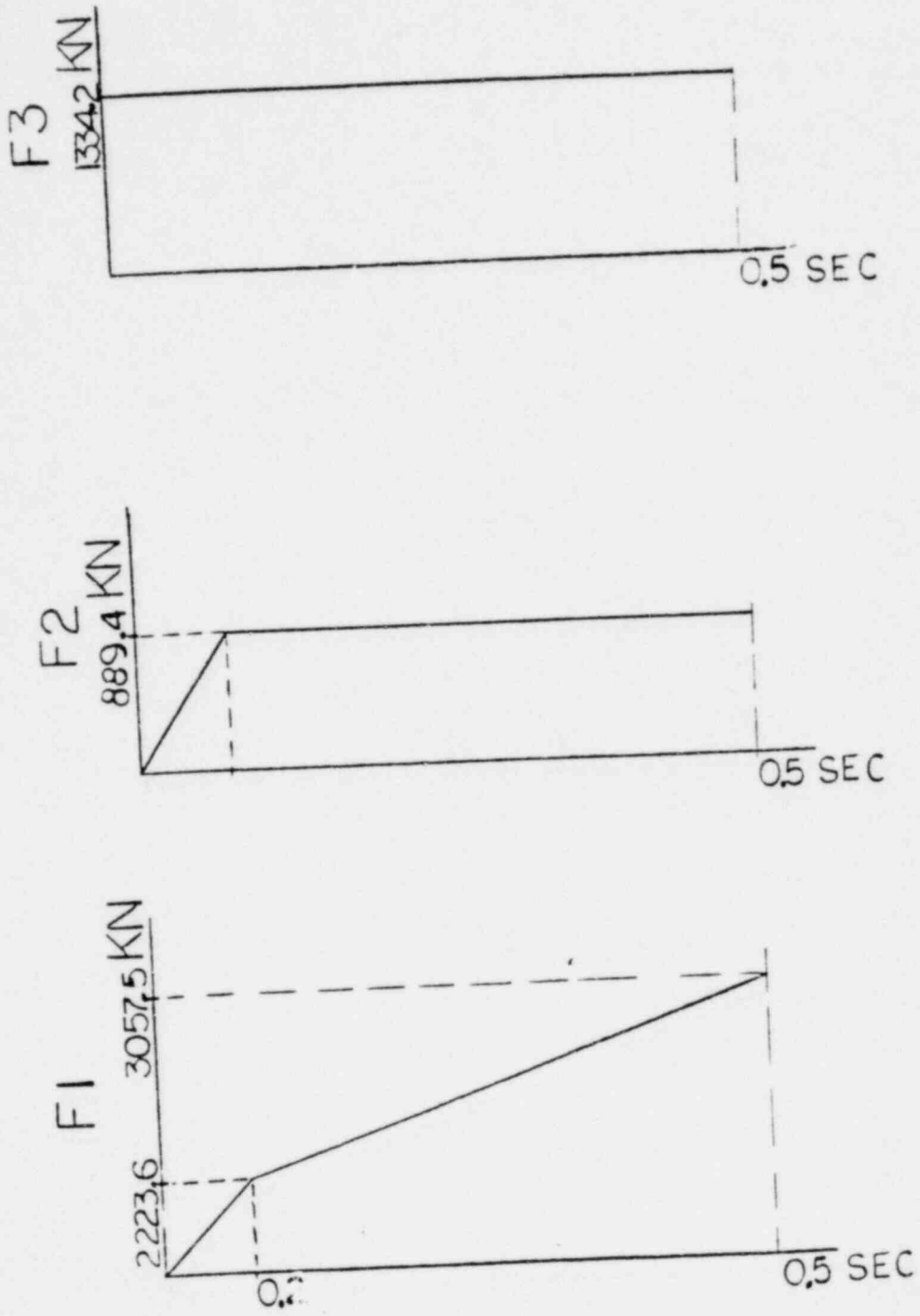

FIG.2 APPLIED FORCING FUNCTIONS

a) Bumper forces 1 (Node 4)

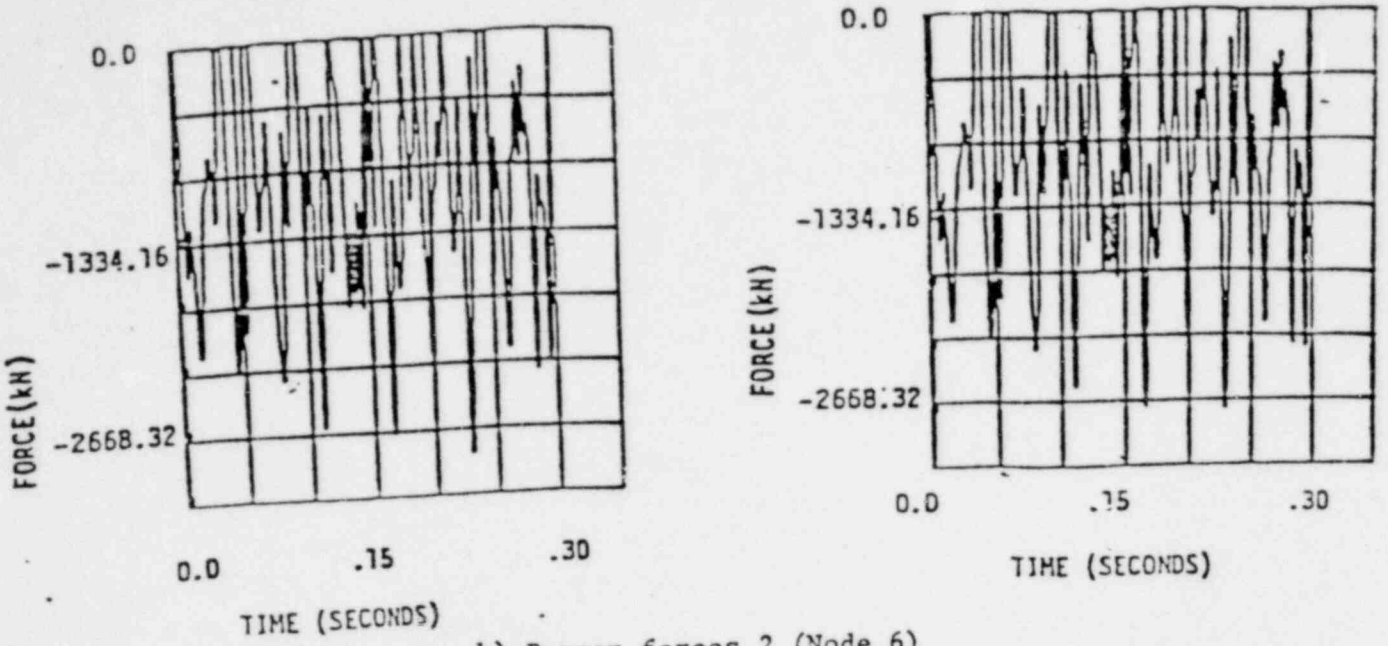

b) Bumper forces 2 (Node 6)

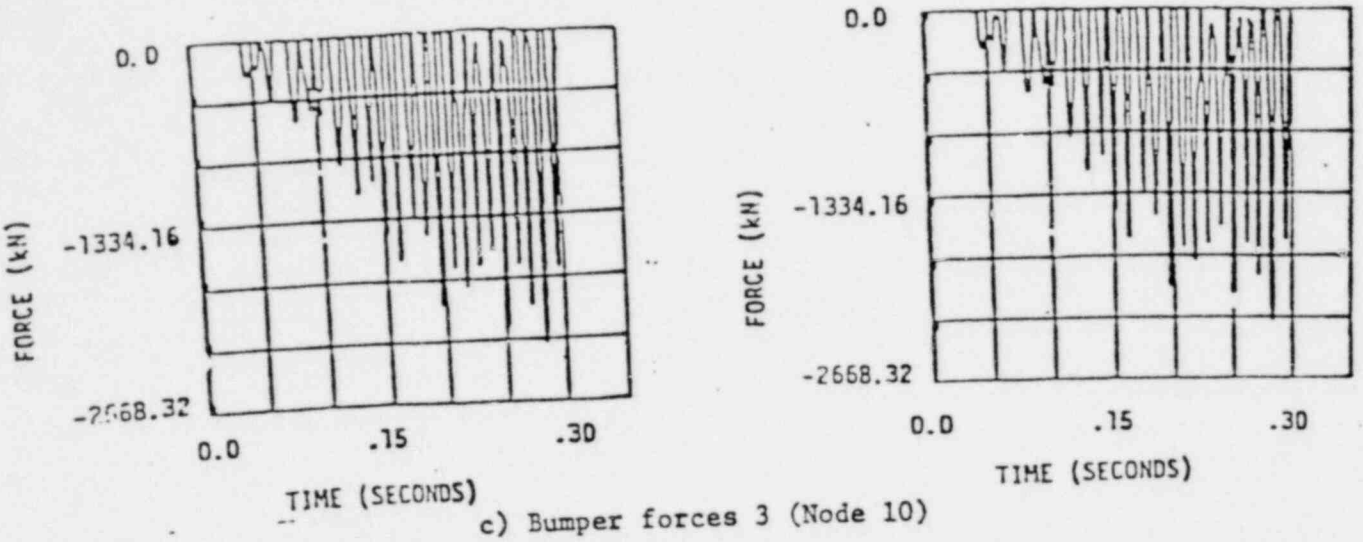

c) Bumper forces 3 (Node 10)

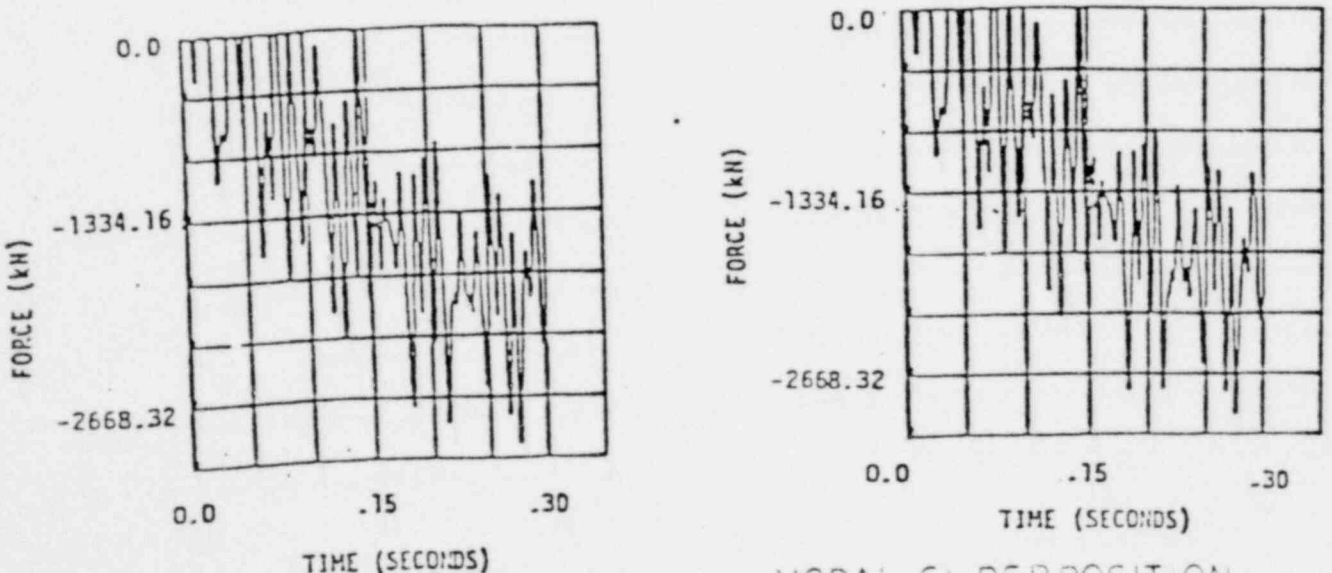

DIPECT INTEGRATION

MODAL SUPERPOSITION

FIG. 3 BUMPER FORCES RESULTS FROM REF. 2

Figures 4, 5, and 6 show the predicted bumper force versus time for each of the bumpers for both the direct integration solution and the modal solution considering 30 modes. In each figure, in fact, three separate solutions for each method are shown, the uppermost corresponding to an integration time step of 0.000125 sec, the center of 0.0000625 sec, and the lower-most to 0.00001325 sec. Figure 4 corresponds to bumper 1 (node 4), Figure 5 to bumper 2 (node 6), and Figure 6 to bumper 3 (node 10) with the direct integration solutions appearing on the left side, the modal solutions on the right.

Comparing the results on any of the Figures indicates that all the solutions look identical. If the numerical results from which the plots were generated are referred to, slight differences are apparent between the solutions for the different time steps and between the modal and direct integration solutions, however, these are all minimal. Referring to the Reference 2, graphical results, Figure 3, again the two sets of graphical output look identical. A comparison of the numerical results to those of Reference 2, show only slight differences.

III.2 Cantilever Beam

As the second example, the response of a cantilever beam subjected to a ground motion acceleration and having two gap-bumper springs at its free end was considered. The identical problem was treated in Reference 5 permitting an evaluation of the results.

The 20 inch long cantilever was modeled with 20 beam elements and 2 gap-bumpers on each side of the free end as shown in Figure 7A. The material and structural properties of the beam were taken as; Young's modulus; 30×10^6, poisson's ratio 0.3; cross-section 2" x 3"; moment of inertia 2 in^4; and mass density 0.0042 $\frac{lb/sec^2}{in}$ per in. The excitation was the ground motion acceleration time history shown in Figure 7B. The gap, G, had an initial clearance

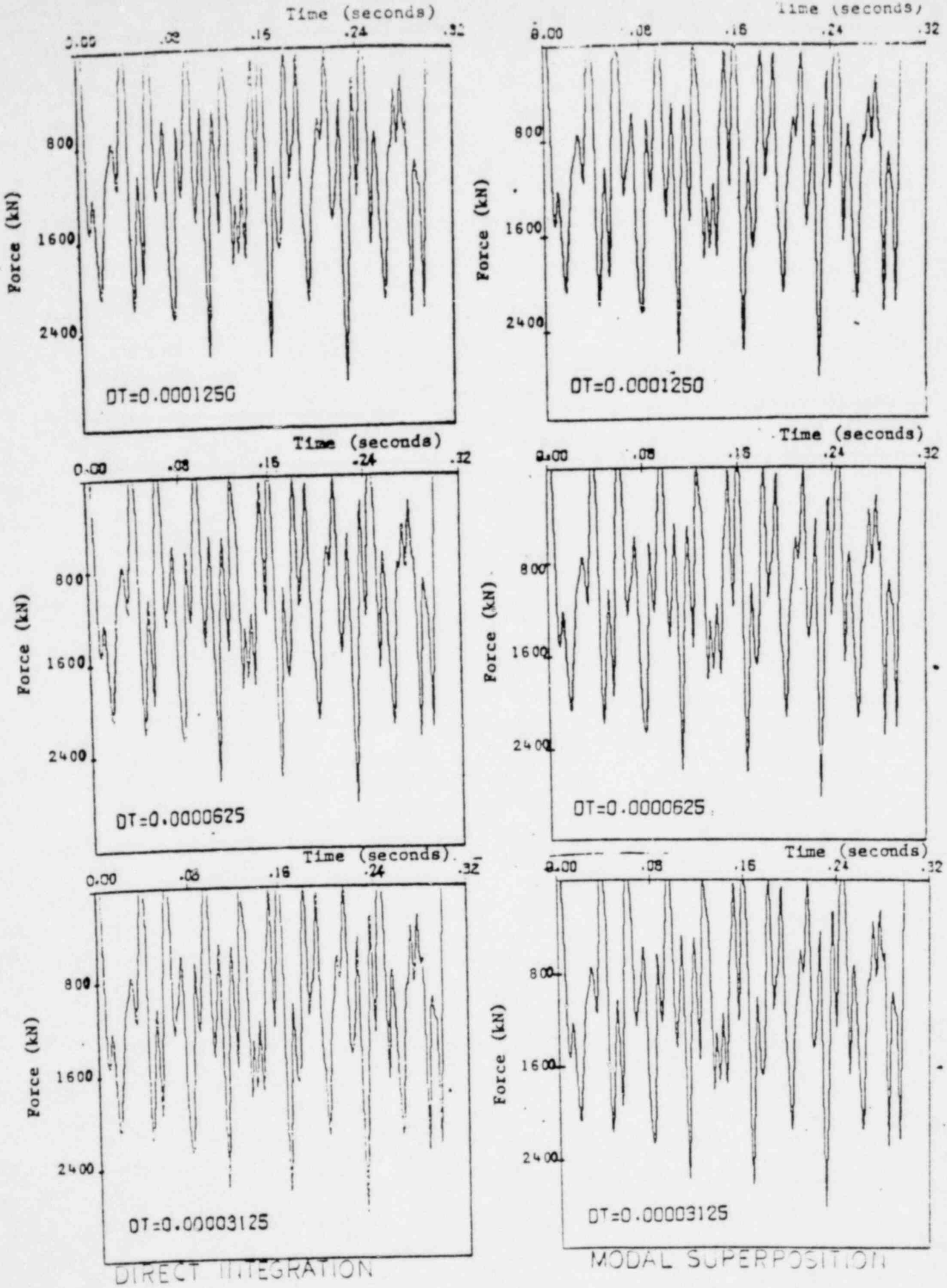

FIG. 4 BUMPER FORCES AT NODE 4

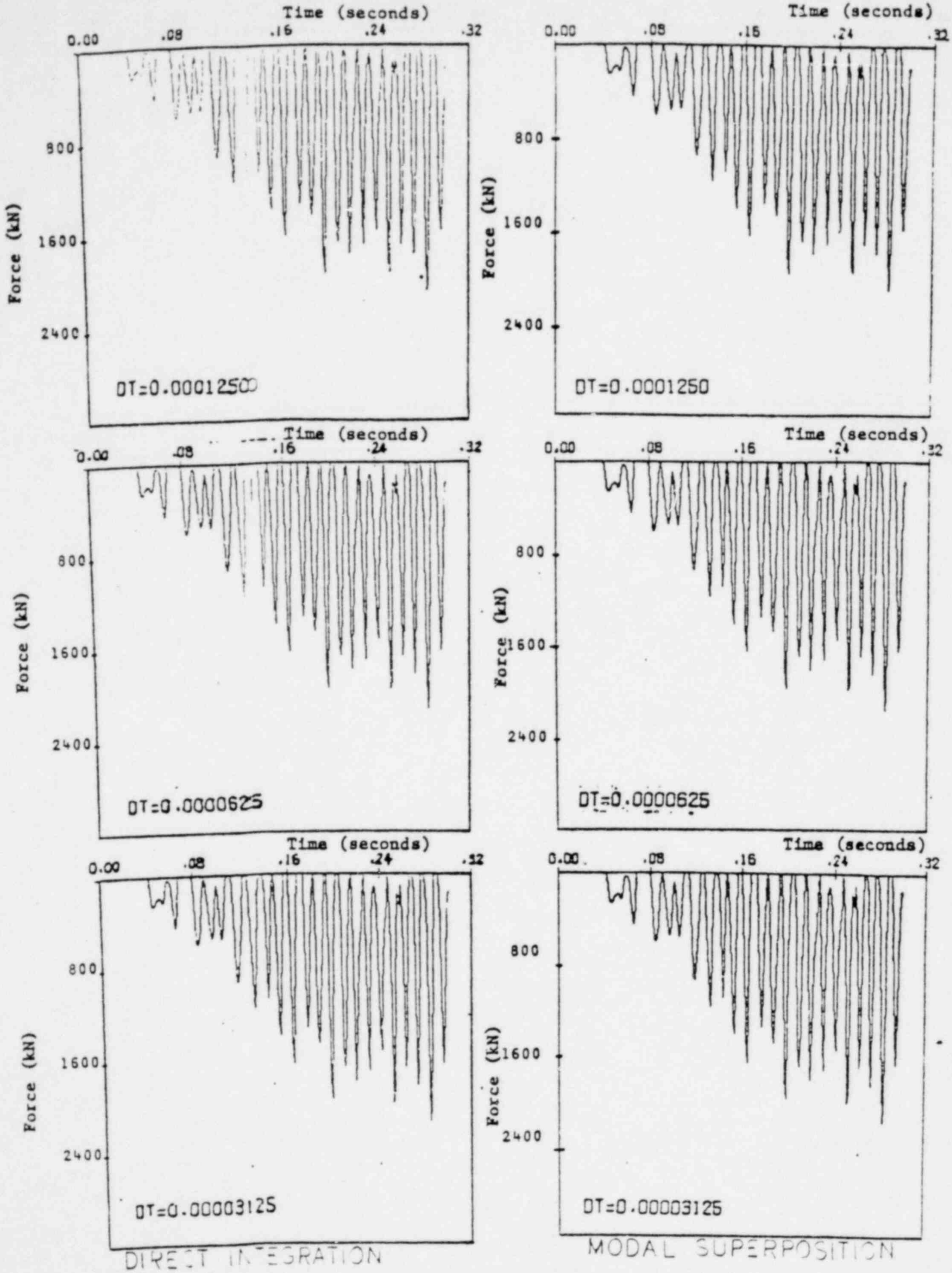

FIG. 5 BUMPER FORCES AT NODE 6

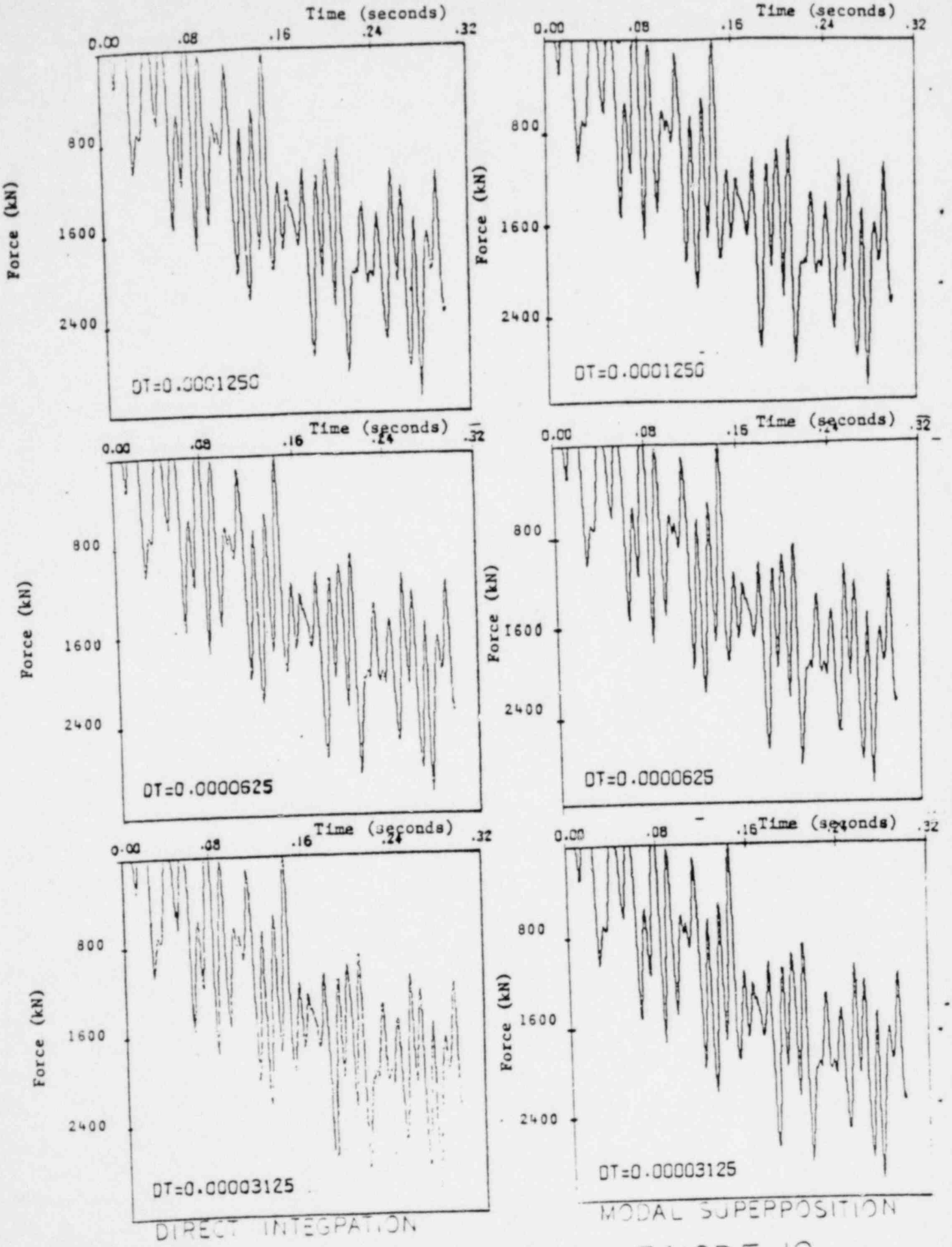

FIG. 6 BUMPER FORCES AT NODE 10

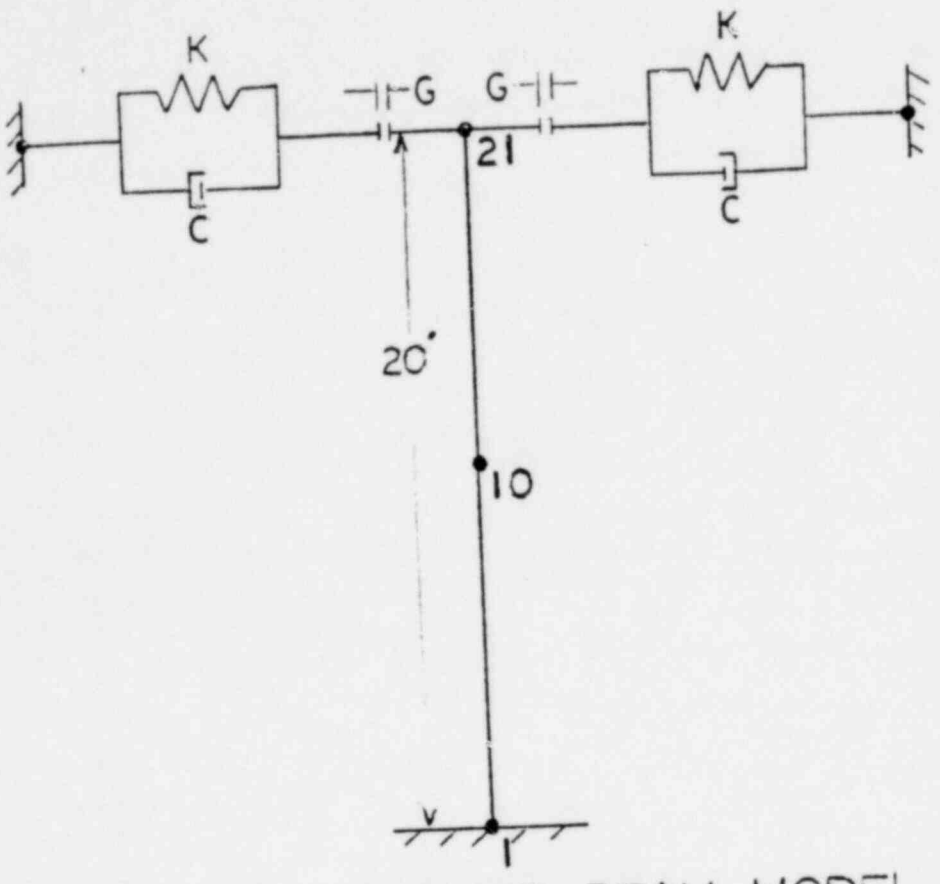

A. THE CANTILEVER BEAM MODEL

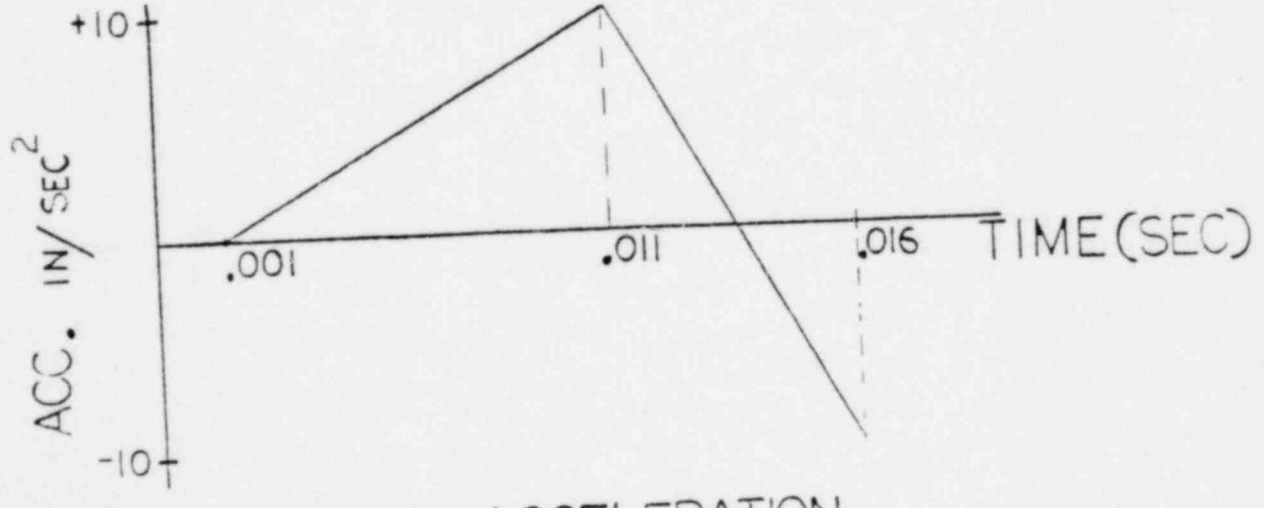

B. GROUND ACCELERATION

FIG. 7

of 0.5×10^5 in; and the bumper spring stiffness, K, was 2×10^5 lb/in. Two cases were considered, in one case the bumper damping coefficient was taken as C = 10.0688 lb/sec/in and the other case was without damping. The time step used in all analyses was 0.00003125 seconds.

The transverse displacement responses determined by direct integration for node 10 and node 21 for both cases are shown in Figure 8 and Figure 9 respectively. The displacement responses for the no damping case from Reference 5 are shown in Figure 10 for comparison. The comparison of Figures 8 and 10 shows good agreement of results. The results for the no damping case indicates that the negative gap-bumper opens and closes three times while the positive gap-bumper opens and closes only once during the event. For the damped case the maximum damping force acts at the beginning and the end of the impact and is zero when the spring force is maximum.

III.3 Concentrated Masses, Ground Motion Excitation

As the third example, a system consisting of three concentrated masses interconnected and attached to ground with linear springs and separated from the side walls with gap-nonlinear spring bumpers, as shown in Figure 11A, was considered. For the analysis, the interelement springs were modeled with truss elements while the linear base springs were modeled with massless beam elements. The bumper elements had an initial gap of 0.001" and a cubic nonlinear spring constant given by

$$k = 1000\ (D-G) + 100{,}000\ (D-G)^3 \qquad (21)$$

The input excitation was the ground motion acceleration time history depicted in Figure 11B. All the pertinent system parameters are shown in Figure 11A.

The response time histories were determined by both the modal superposition method and direct integration using an integration time step of 0.001 sec.

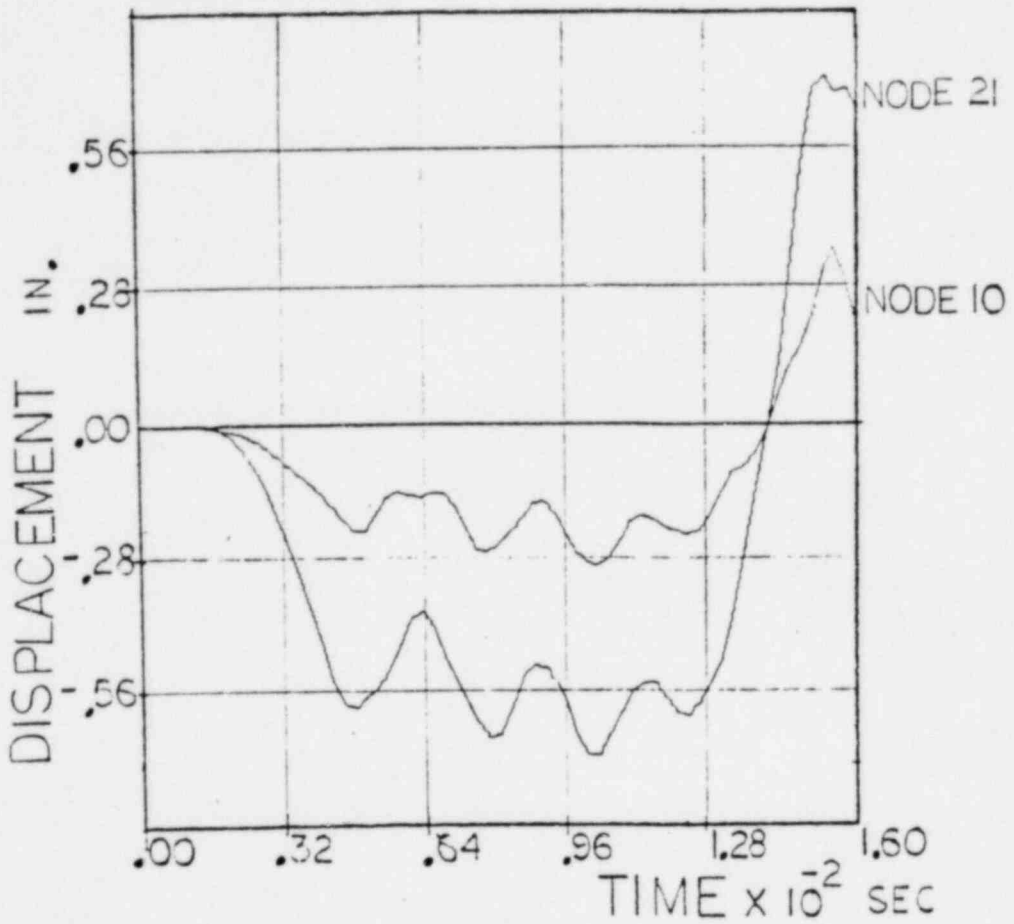

FIG.8 DISPLACEMENT TIME HISTORY
MODEL W/O DAMPING

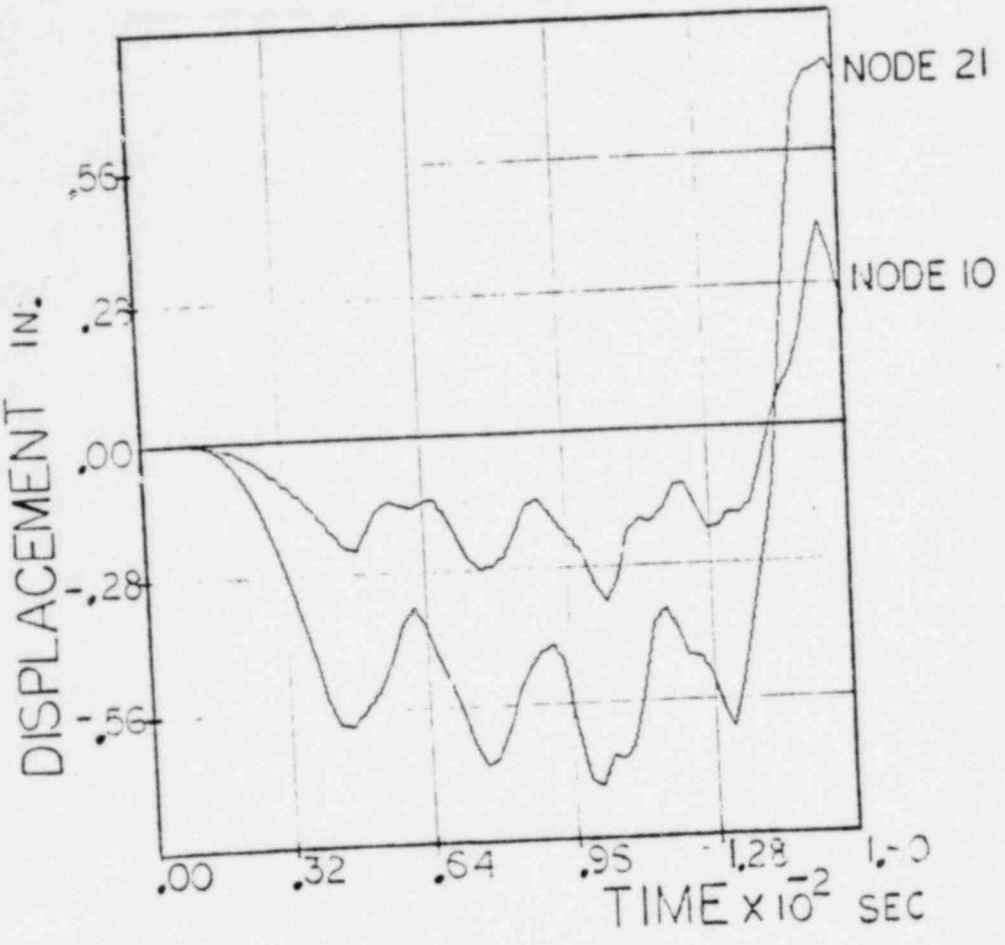

FIG. 9 DISPLACEMENT TIME HISTORY MODEL WITH DAMPING

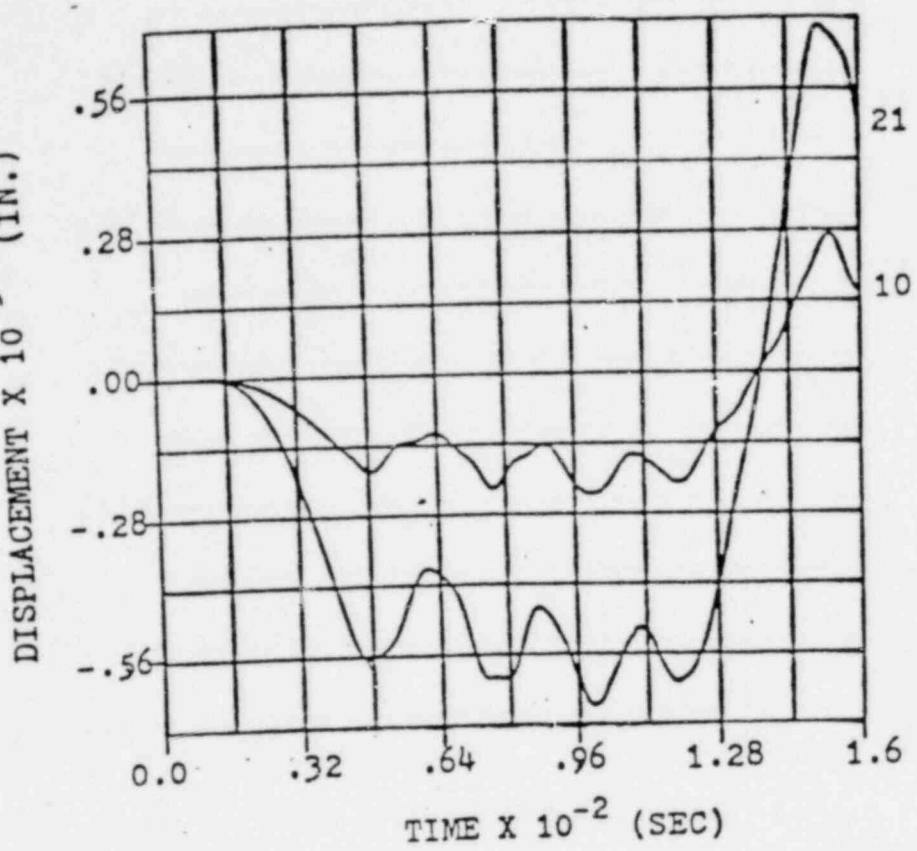

FIG. 10 DISPLACEMENT TIME HISTORY MODEL W/O DAMPING (FROM REF.5)

A. 3-MASSES SYSTEM

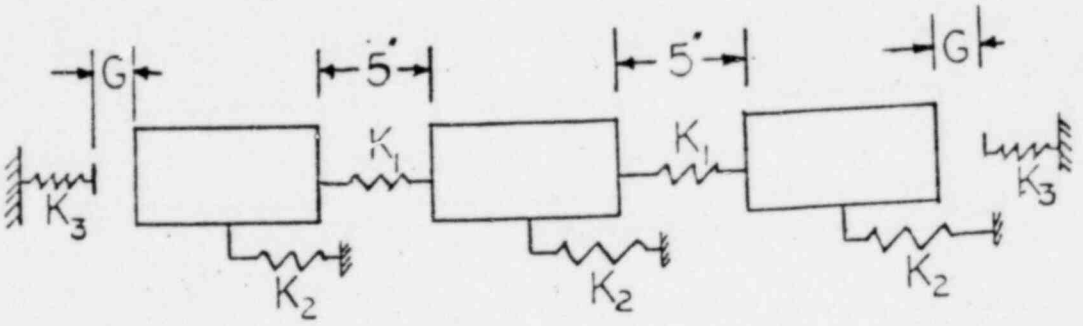

K_1 = 10000 Lb/IN

K_2 = 18 Lb/IN

K_3 = $1000(D-G) + 100000(D-G)^3$

D = NODAL DISPLACEMENT HISTORY

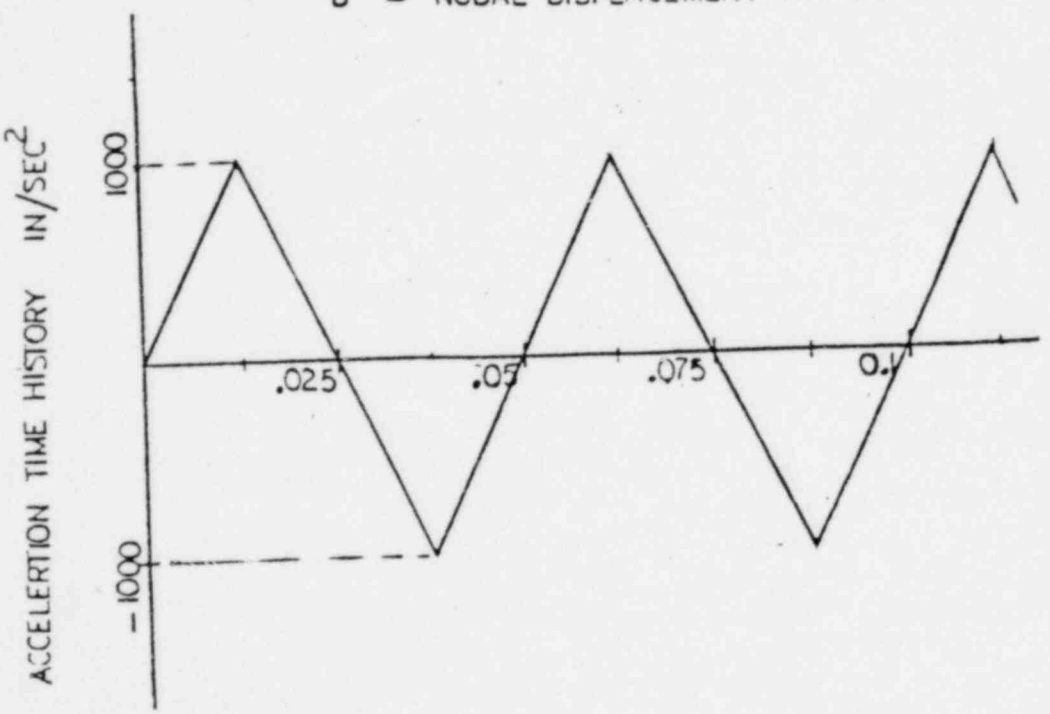

B. GROUND ACCELERATION

FIG. 11

To provide a means to corroborate the results, the system response was also determined using the BNL nonlinear dynamics code OSCIL (Reference 6). This code, developed to evaluate HTGR core block response, is designed to evaluate the response of multimass systems containing nonlinear spring elements with general characteristics. It incorporates a numerical integration scheme which automatically varies the integration time step size as a function of event severity.

The resultant displacement time histories for the three masses are shown in Figures 12A and 12B with the modal superposition results shown in A and the direct integration results in B. The predicted bumper force time histories for both methods are shown in Figures 13A and 13B, with the positive forces corresponding to the left side bumper and the negative forces corresponding to the right side bumper. The OSCIL predicted displacement time histories are shown in Figure 12C and the corresponding bumper force time histories are shown in Figure 13C.

A comparison of Figures 12A, 12B, and 12C or 13A, 13B and 13C indicates that all three methods provide near identical results. A comparison of the numerical results for the three runs showed minimal differences with the best agreement occurring between the direct integration solution and the OSCIL results. Additional direct integration runs with finer time steps produced further convergence to the OSCIL solution

III.4 Concentrated Masses, Sweeping Sinosoidal Excitation

As a last test of the method, the three mass problem was again used to investigate whether the psuedo force method would correctly predict the multiple response roots inherent in this nonlinear system. Using the direct integration solution mode and the OSCIL code, the response of the system to a sweeping frequency sinusoidal forcing function, the frequency being both swept up and

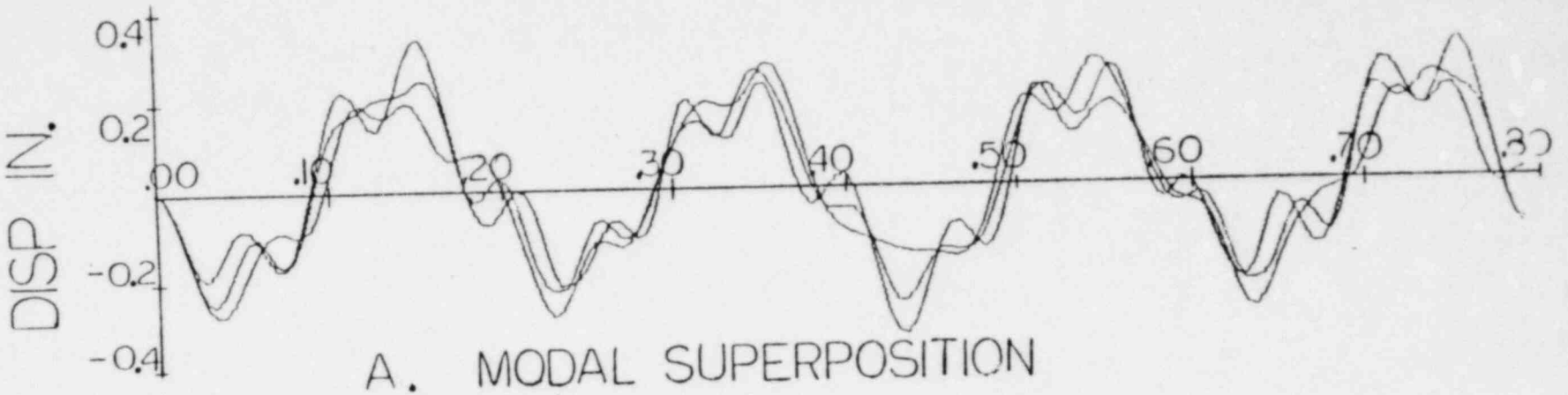

A. MODAL SUPERPOSITION

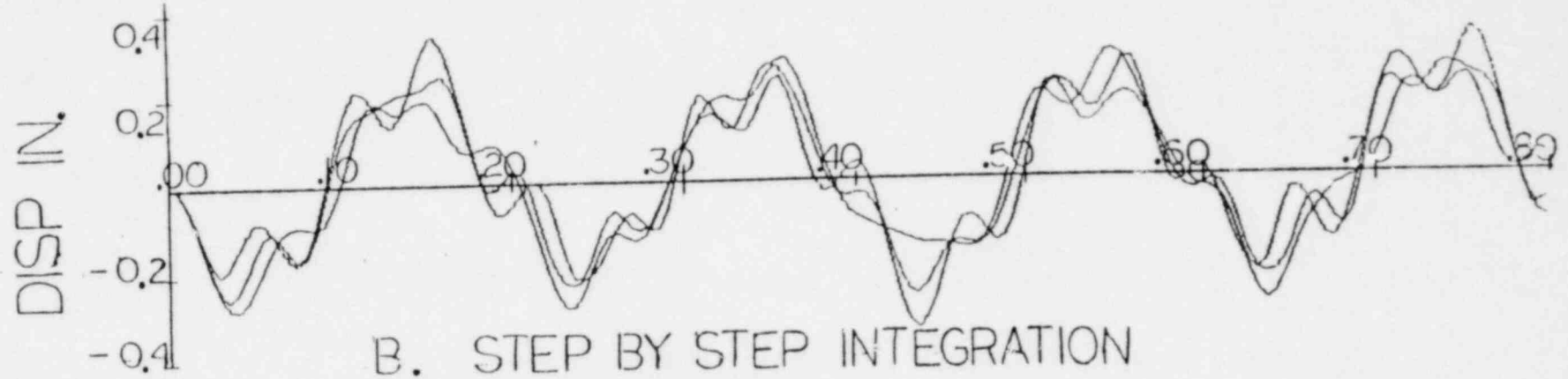

B. STEP BY STEP INTEGRATION

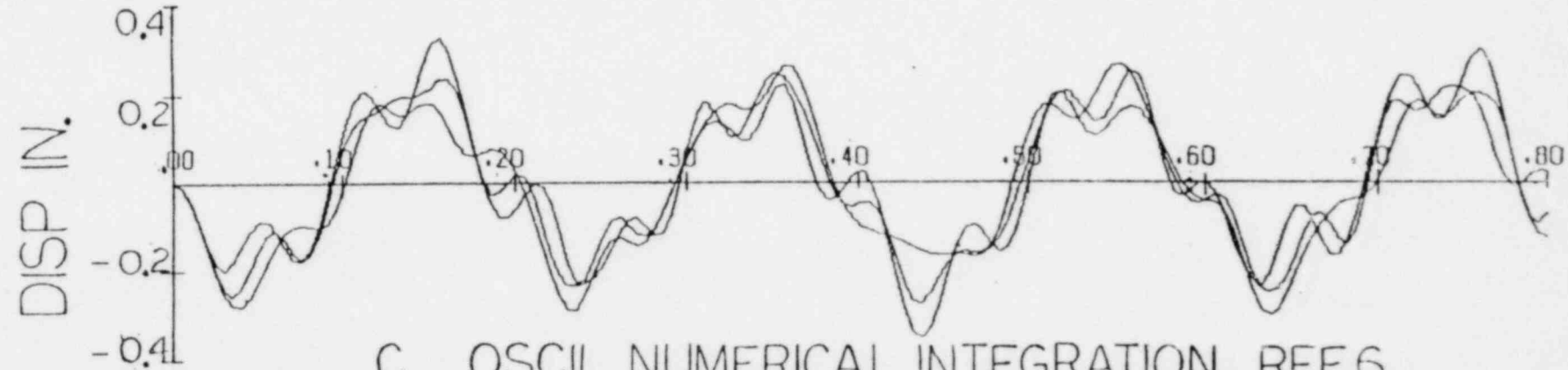

C OSCIL NUMERICAL INTEGRATION REF.6

FIG.12 DISPLACEMENT TIME HISTORY

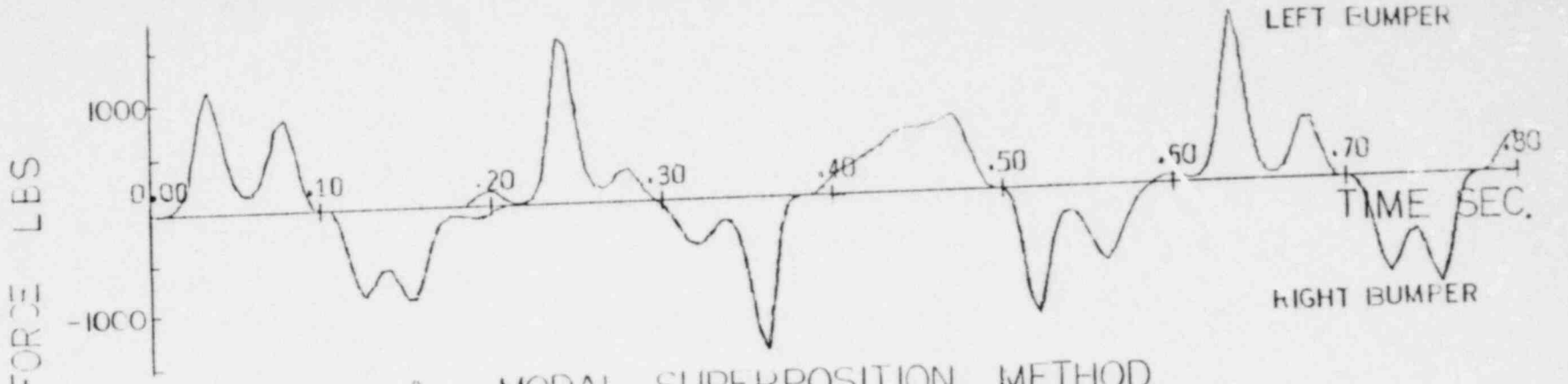

A. MODAL SUPERPOSITION METHOD

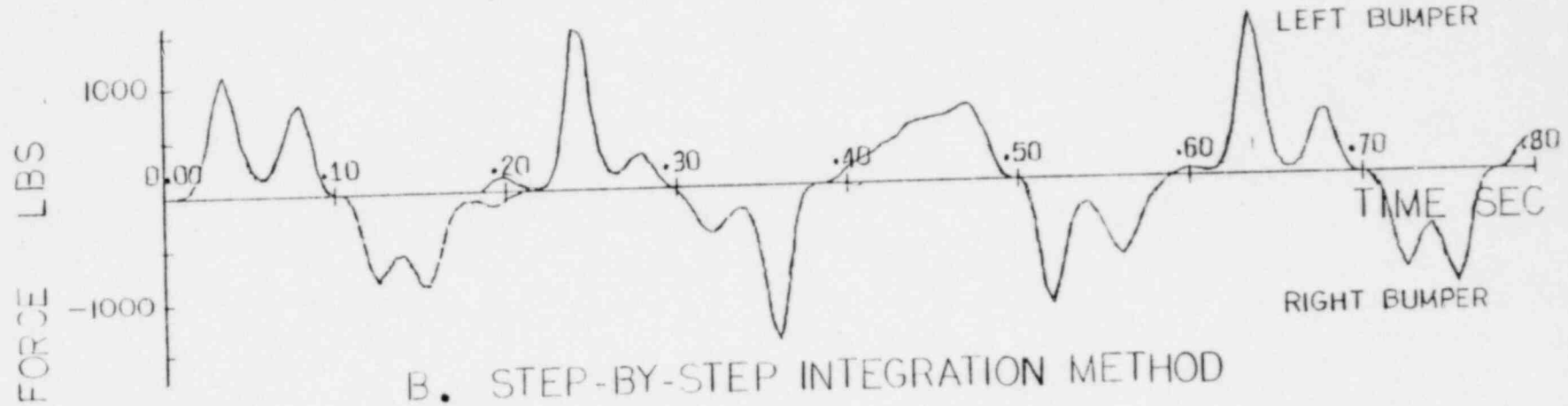

B. STEP-BY-STEP INTEGRATION METHOD

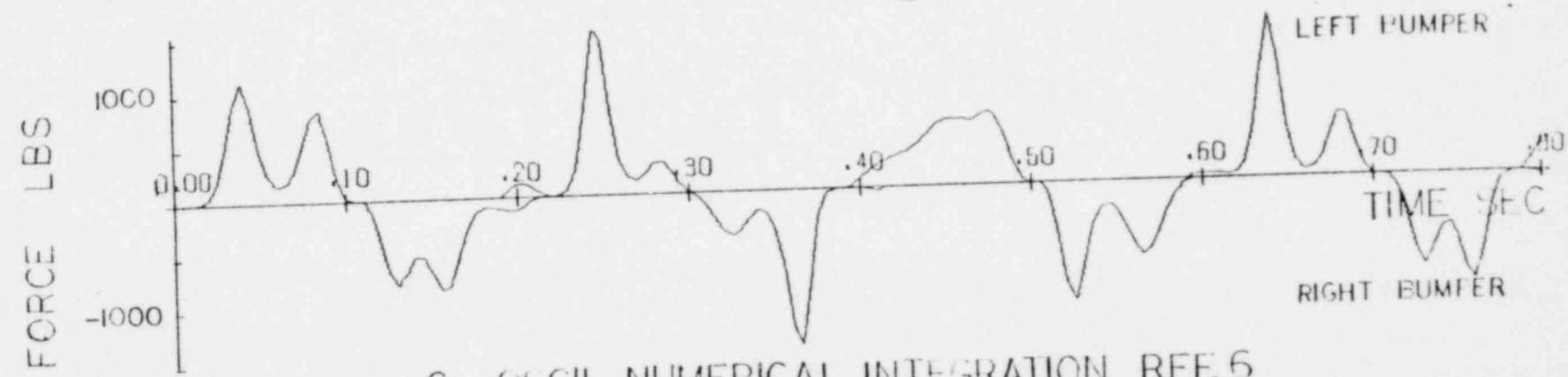

C. OSCIL NUMERICAL INTEGRATION REF. 6

FIG 13 BUMPER FORCES

swept down, was determined. The excitation was a concentrated force given by $F=20\cos(\omega t)$ acting, in phase, on each mass point. For the direct integration solution the integration time step was 1×10^{-4} seconds while the OSCIL code adapted minimum time steps as small as 1×10^{-5} seconds.

Both solution methods predicted the same response curve, shown in Figure 14. This curve is typical for a system with a hardening characteristic [5] and was to be expected for the problem being considered. In the frequency range 4→6 cps two distinct response roots are evident, the root exhibited by the system excited at these frequencies being determined by the prior history transients. Clearly, this result further confirms the adequacy of the psuedo force method as a nonlinear analysis method.

IV. Conclusions

The implementation of the psuedo force method into an existing elastic finite element code was found to be straightforward. The required modifications were most readily made for the direct integration solution mode while requiring some additional coding for the modal superposition solution mode (gap effects necessitated a constant return to system coordinates). Lastly, potential problems foreseen for the development of a pseudo force iteration scheme proved unfounded as the simplest, most direct procedure provided acceptable accuracy.

Concerning the problem solutions contained herein, the results predicted with the BNL psuedo force code option agreed in all important aspects with the existing solutions. This was true for both the direct integration and the modal superposition solution modes with the latter exhibiting slightly greater, but insignificant, inaccuracys. As with linear system analyses, the modal superposition solution mode was found to be the most rapid, exhibiting the reduction in computer running time normally associated with it.

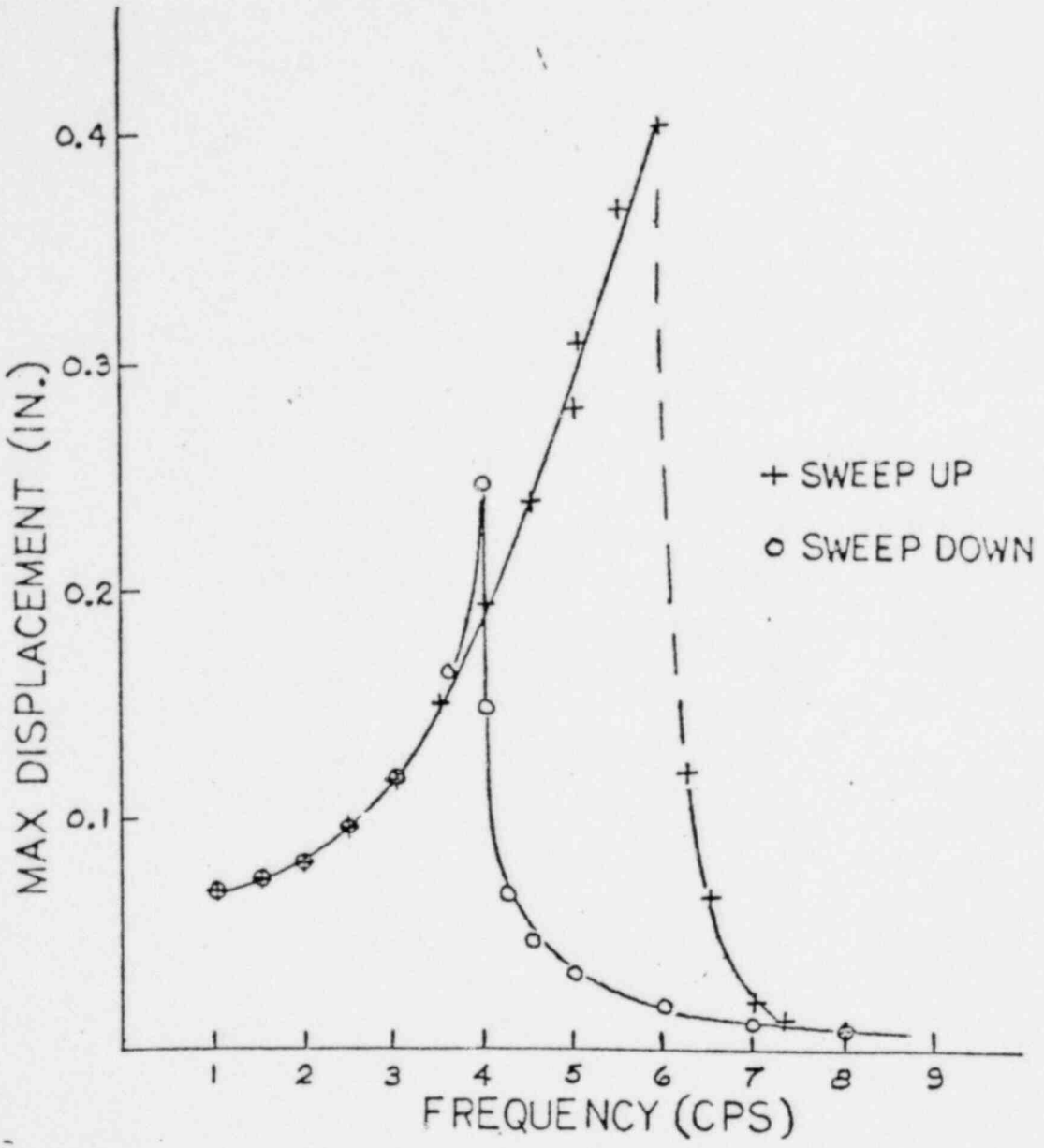

FIG. 14 RESPONSE 3 MASS SYSTEM

The psuedo force method was found to be a fully general nonlinear analysis method. Its employment for the analysis of linear systems containing a limited number of discrete nonlinear components is recommended as it is both more economical and as accurate as more sophisticated nonlinear methods. However, since these advantages rapidly decline as either the extent or duration of nonlinear affects increase it is not recommended as a general purpose nonlinear method.

LIST OF FIGURES

References

1. Stricklin, J. A., Haisler, W. E., and Von Riesmann, W. A., "Computation and Solution Procedures of Nonlinear Analysis by Combined Finite Element-Finite Difference Methods", Computer and Structures, Pergamon Press, Vol. 2, pp. 955-974, 1972.

2. Molnar, A. J., Vashi, K. M., and Gay, C. W., "Application of Normal Mode Theory and Pseudo Force Methods to Solve Problems with Nonlinearities", J. of Pressure Vessel Technology, pp. 151-156, May 1976.

3. Belytschko, T., "A Survey of Numerical Methods and Computer Programs for Dynamic Structural Analysis", Nuclear Engineeering and Design Vol. 37, pp. 23-24, 1976.

4. Bathe, K. J., "Numerical Methods in Finite Element Analysis", Prentice-Hall, 1976.

5. Shah, V. N., Nahavandi, A. N., and Bohn, G. J., "Modal Superposition Method for Computationally Economical Nonlinear Structural Analyses", To be presented in 1978.

6. Lasker, L., et al., "OSCIL: One Dimensional Spring-Mass System Simulator for Seismic Analysis of HTGR Cores", BNL 21023, January 1976.